Kerr noise reduction and squeezing

Andrew G White†§, Ping Koy Lam‡, David E McClelland‡, Hans-A Bachor‡ and William J Munro†

† Department of Physics, University of Queensland, Brisbane, Queensland 4072, Australia
‡ Department of Physics, Australian National University, Canberra, ACT 0200, Australia
§ Physics Division, P-23, Los Alamos National Laboratory, Los Alamos, NM 87545, USA

Abstract. We introduce a model of squeezing and noise reduction in the Kerr effect that accounts for noise in all quadratures of the driving field. Consequently we show that Kerr squeezing is much more sensitive to driving noise than squeezing produced by second harmonic generation (SHG). We experimentally demonstrate this sensitivity using a nonlinear system that tunes between strong classical SHG and Kerr behaviours. Whilst the system experiences strong squeezing in the SHG limit, it experiences no squeezing in the Kerr limit, although it does experience strong classical noise reduction, or 'classical squeezing'.

1. Introduction

It is now well over a decade since squeezed light was first demonstrated [1]. In that time, many nonlinear processes have been investigated for their suitability as sources of squeezed light‖. With interest now moving from the production of squeezing to its application [2] attention has moved away from demonstration experiments towards producing robust, well-understood sources of squeezing.

In the pulsed regime the potential for intrinsically robust squeezing sources is high, with up to 5.1 dB/69% of squeezing observed [3–5] in relatively straightforward systems. In the cw regime the situation is more complicated: there are a number of suitable nonlinear processes, both active and passive, not all of which have yet attained their full potential as robust sources of strongly squeezed bright light. The most successful *active* cw systems to date have been diode lasers: in recent years squeezing of up to 2.3 dB/41% has been observed [6]. In the medium term diode lasers offer the possibility of 'key-turn' sources of moderate squeezing: the current limitations are in understanding and suppressing the various noise processes of these systems (polarization, side modes, etc) [6, 7], and in the material manufacturing, so that larger degrees of squeezing are possible at room temperature.

Three *passive* nonlinear systems have been widely employed to make cw squeezed light: optical parametric oscillation/amplification (OPO/A); second harmonic generation (SHG); and the Kerr effect. Parametric amplification has enjoyed great success both as a source of cw vacuum squeezing (7.0 dB/80% observed [8]), and as a source of 'bright' squeezing (up to 6.2 dB/76% observed at 200 μW [9]¶).

Unfortunately OPO/A systems are technically complicated: three nonlinear components are required (the pump laser, frequency doubler and parametric amplifier) all of which must be locked together to produce stable operation. SHG is more robust: only the laser and SHG crystal are required. To date SHG is the best understood source of bright cw squeezed light: models have been developed that account for the effect of the driving field noise [12, 13], by reducing this noise 2.2 dB/40% squeezing at 30 mW has been observed, in exact agreement with theory [13]. Higher values of squeezing have been demonstrated in SHG (up to 4 dB/60% [14]): by building such a system in a Sagnac cavity to cancel the pump noise [3, 15] it should be possible to achieve large squeezing in a robust system.

The final nonlinear process widely employed to produce bright cw squeezing is the Kerr effect⁺, which in principle is as robust as SHG. Whilst the Kerr effect has enjoyed great success in the pulsed regime (up to 5 dB squeezing [3]), it has been employed less successfully in the cw, with up to 2.2 dB/40% squeezing observed [16]. Partly, this is due to difficulty of achieving strong third-order nonlinearities: in solid state systems the low nonlinearity necessitates very high pump powers, typically achieved via pulsing; stronger nonlinearities can be achieved in atomic systems, but these are intrinsically complicated, requiring a build-up cavity placed around either an atomic beam or trap [16–18]. Aside from the difficulty of achieving a strong nonlinearity, it is also possible that part of the discrepancy between predicted and achieved outcomes is that the predictions do not properly account for the effects of driving noise (as proved to be

---

‖ For example, see the summary of squeezing experiments in [23].
¶ Of course vacuum squeezing can always be combined with a coherent field via a cavity [10] or a beamsplitter [11] to produce bright squeezing, but typically this adds many extra components and/or wastes power.

⁺ Although strictly speaking an intensity-dependent refractive index, in quantum optics the phrase 'Kerr effect' has come to refer to a variety of third-order processes where the light experiences an intensity-dependent phase shift.

the case for SHG squeezing). It is this possibility that we investigate in this paper.

There have been various treatments of the noise behaviour of a Kerr medium in a cavity [16–21]. All have considered only the case of a quantum noise limited driving field, and are thus of limited utility for modelling and understanding many experiments. We find that, as expected from phenomenological arguments, the squeezing and noise reduction behaviour is influenced by the noise in both the amplitude and phase quadratures of the driving field, unlike SHG, which in the optimum case is sensitive only to the amplitude quadrature.

2. Theory

The conceptual layout of the system we model is shown in figure 1. The Kerr medium resides in an optical build-up cavity. Ideally, the cavity loss is zero and the reflected driving field is optimally squeezed without loss of power, however, this is rarely the case in practice. Accordingly, we consider two ports for the cavity: the coupling port, 1, through which the cavity is driven by a steady-state field of frequency ν_1; and an 'other' port, 2, representing cavity loss, transmission, etc (no power enters through this port, only quantum noise). The equations of motion for such a system are

$$\dot{\hat{a}}_1 = -(\gamma_1 + i\Delta_1)\hat{a}_1 \pm i\mu \hat{a}_1^\dagger \hat{a}_1 \hat{a}_1 + \sqrt{2\gamma_1^c}\,\hat{A}_1^{\text{in1}} + \sqrt{2\gamma_1^\ell}\,\hat{A}_1^{\text{in2}} \quad (1)$$

and its conjugate equation. The first term represents linear loss and detuning; the second term, nonlinear detuning due to the Kerr effect. Classical power asymmetries occur when the nonlinear and linear detunings have opposite sign; bistability occurs when the magnitude of the nonlinear term is equal to or greater than that of the linear [22]. The third and fourth terms of equation (1) are the driving terms. The driving fields at each port are represented by the operators $\hat{A}^i$ and $\hat{A}^{\dagger i}$; the intracavity mode by the dimensionless operators $\hat{a}$ and $\hat{a}^\dagger$; μ is the nonlinear coupling constant; γ_1^c is the decay rate of the coupling port; γ_1^ℓ is the decay rate of the loss port; and $\gamma_1 = \gamma_1^c + \gamma_1^\ell$ is the total decay rate of the cavity. The escape efficiency of the cavity is defined as $\eta = \gamma_1^c/\gamma_1$: we explicitly consider two ports so that we can model the experimental situation of imperfect escape efficiency, $\eta < 1$.

At this point it is possible to build up an intuitive understanding of the squeezing mechanism due to the Kerr nonlinearity. It is clear from equation (1) the Kerr effect acts as an intensity dependent phase shift. That is, the stronger the field, the proportionately larger the phase shift. Now consider the phasor, or 'ball-on-stick' picture [23] of the light inside the cavity, as shown in figure 2. The amplitude of the light is rotated by an angle proportional to the square of the amplitude ($\mu|\alpha_1|^2$). The uncertainty area is also affected: the top of the ball (the point furthest from the origin) is rotated further than the bottom of the ball (the point closest to the origin) as it is of greater power. The uncertainty area is thus smeared out into a banana or teardrop shape as shown in figure 2. Note that for some quadrature angles the uncertainty is less than that originally—the light is now squeezed. Obviously then, squeezing via the Kerr effect is sensitive to both amplitude (length of the the phasor) and phase (angle of the phasor) fluctuations.
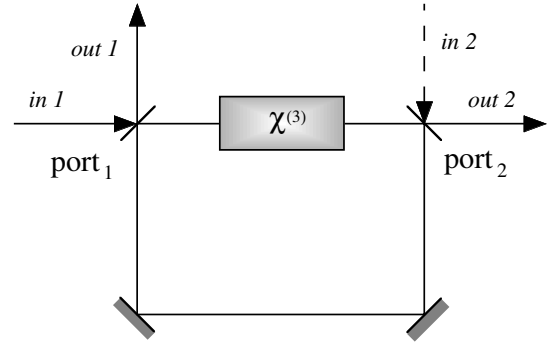
Figure 1. Conceptual layout of system. Solid lines represent fields with non-zero average values, broken lines indicate vacuum fields. Port 1 is the coupling port: in 1 is the driving field at frequency ν_1, out 1 is the reflected driving field. Port 2 is the port representing undesired cavity loss, transmission, etc: in 2 is the vacuum input, out 2 the transmitted field and reflected vacuum input.
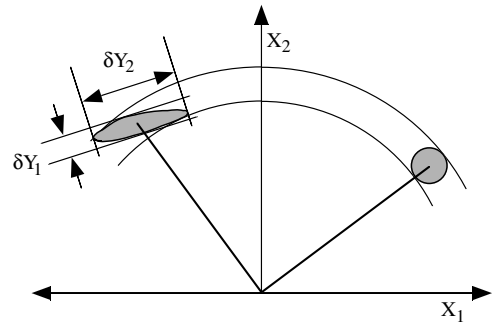

Figure 2. Intuitive explanation of Kerr squeezing. Phasor diagrams for an intracavity fundamental field: right-hand side without Kerr effect; left-hand side with Kerr effect. The top of the uncertainty area is more intense than the bottom, and so is phase shifted further by the Kerr effect. The uncertainty area is now narrower at some quadrature angles then the original area—at these quadrature angles the light is squeezed.

To see this formally, we linearize equation (1) in the standard manner [23,24]. We consider the rotated quadrature operators, $\hat{Y}_1$ and $\hat{Y}_2$, where

$$\begin{aligned} \hat{Y}_1 &= \hat{a}e^{-i\theta} + \hat{a}^\dagger e^{+i\theta} \\ \hat{Y}_2 &= -i(\hat{a}e^{-i\theta} - \hat{a}^\dagger e^{+i\theta}) \end{aligned} \quad (2)$$

where θ is the quadrature angle. For $\theta = 0$, $\hat{Y}_1 = \hat{X}_1$ and $\hat{Y}_2 = \hat{X}_2$, where $\hat{X}_1$ and $\hat{X}_2$ are respectively the amplitude and phase quadratures. The quadrature fluctuation equations of motion are thus

$$\delta\dot{\hat{Y}}_i = G\delta\hat{Y}_i + H_i\delta\hat{Y}_j + J_i \quad (3)$$

where the subscripts $i = 1, 2$ and $j = 2, 1$ denote the quadrature and its complement; and G and H are defined as

$$G = -\left(\gamma_1 - i\frac{\mu}{2}[\alpha_1^2 e^{-i\theta} - \alpha_1^{*2}e^{+i\theta}]\right) \quad (4)$$

$$H_i = \pm(\Delta_1 - 2\mu|\alpha_1|^2) + \frac{\mu}{2}[\alpha_1^2 e^{-i\theta} + \alpha_1^{*2}e^{+i\theta}]) \quad (5)$$

where the variable sign of the nonlinear term has been absorbed into the nonlinear constant, μ; the '+' sign indicates

H_1; and the '$-$' sign indicates H_2. J_i is the coupling term

$$J_i = \sqrt{2\gamma_1^c}\,\delta\hat{Y}_i^{\text{in1}} + \sqrt{2\gamma_1^\ell}\,\delta\hat{Y}_i^{\text{in2}}. \qquad (6)$$

Fourier transforming equation (3) and eliminating the cross terms we obtain the expressions

$$\delta\tilde{Y}_i = \frac{H_i J_j - J_i(G + i\omega)}{(G + i\omega)^2 - H_i H_j}, \qquad (7)$$

where the tilde represents a Fourier transformed fluctuation operator. We are interested in the reflected driving field, the boundary condition for this field is

$$\tilde{Y}_i^{\text{out1}} = \sqrt{2\gamma_1^c}\,\tilde{Y}_i - \tilde{Y}_i^{\text{in1}}. \qquad (8)$$

Applying this to equation (7) and taking the self-correlations we obtain the noise spectrum for the reflected driving field

$$V_{Y_i}^{\text{out1}}(\omega) = \Bigg(|(G + i\omega)(2\gamma_1^c + (G + i\omega)) - H_i H_j|^2 V_{Y_i}^{\text{in1}}(\omega)$$

$$+ 4\gamma_1^{c2}|H_i|^2 V_{Y_j}^{\text{in1}}(\omega) + 4\gamma_1^c\gamma_1^\ell(|G|^2 + \omega^2)V_{Y_i}^{\text{in2}}(\omega)$$

$$+ |H_i|^2 V_{Y_j}^{\text{in2}}(\omega)\Bigg) \Big/ \left\{|(G + i\omega)^2 - H_i H_j|^2\right\}. \qquad (9)$$

As port 2 represents loss, transmission etc, no driving field enters via it: in noise terms it is a vacuum input, i.e. $V_{Y_{i,j}}^{\text{in2}}(\omega) = 1$.

2.1. Limits to noise reduction

For any observation quadrature (i.e. any value of θ), the noise on the reflected driving field is given by equation (9). The equation is too complicated to see obvious regimes and limits of squeezing by inspection (unlike the similar equations that account for driving noise in the case of SHG [13, 25]). Fortunately appropriate choice of observation quadrature simplifies the expressions somewhat, so that they depend only on the absolute magnitude of the mode, $|\alpha_1|$. If we observe at the quadrature angle $\theta = 2\psi$†, where ψ is the argument of the intracavity mode, $\alpha = |\alpha|e^{i\psi}$, the spectra for the two quadratures, Y_1 and Y_2 become

$$V_{Y_{1,2}}^{2\psi}(\omega) = \Bigg([\omega^2 - (2\acute{c} + 1) - (\acute{\Delta} - \acute{n})(\acute{\Delta} - 3\acute{n})]^2 V_{Y_{1,2}}^{\text{in1}}(\omega)$$

$$+ 4\acute{\omega}^2(\acute{c} + 1)^2 V_{Y_{1,2}}^{\text{in1}}(\omega) + 4\acute{c}^2(\acute{\Delta} - \acute{n})^2 V_{Y_{2,1}}^{\text{in1}}(\omega)$$

$$+ 4\acute{c}\acute{\ell}(\acute{\omega}^2 + 1)V_{Y_{1,2}}^{\text{in2}}(\omega) + (\acute{\Delta} - \acute{n})^2 V_{Y_{2,1}}^{\text{in2}}(\omega)\Bigg) \Big/$$

$$\left\{[(\acute{\Delta} - \acute{n})(\acute{\Delta} - 3\acute{n}) - \omega^2 + 1]^2 + 4\omega^2\right\} \qquad (10)$$

where we have introduced the scaled quantities

$$\acute{\omega} = \frac{\omega}{\gamma_1} \qquad \acute{\Delta} = \frac{\Delta_1}{\gamma_1} \qquad \acute{n} = \frac{\mu|\alpha_1|^2}{\gamma_1}$$

$$\acute{c} = \frac{\gamma_1^c}{\gamma_1} \qquad \acute{\ell} = \frac{\gamma_1^\ell}{\gamma_1} \qquad (11)$$

where $\acute{n}$ is the degree of nonlinearity and $\acute{c}$ is the coupling ratio. By inspection, the maximum squeezing occurs when

† Note that if we observe at the quadrature angle $\theta = 2\psi \pm \pi/2$ we see no squeezing in either Y_1 or Y_2 as at those quadrature angles $H_1 = -H_2$ so that $V_{Y_1} = V_{Y_2}$.
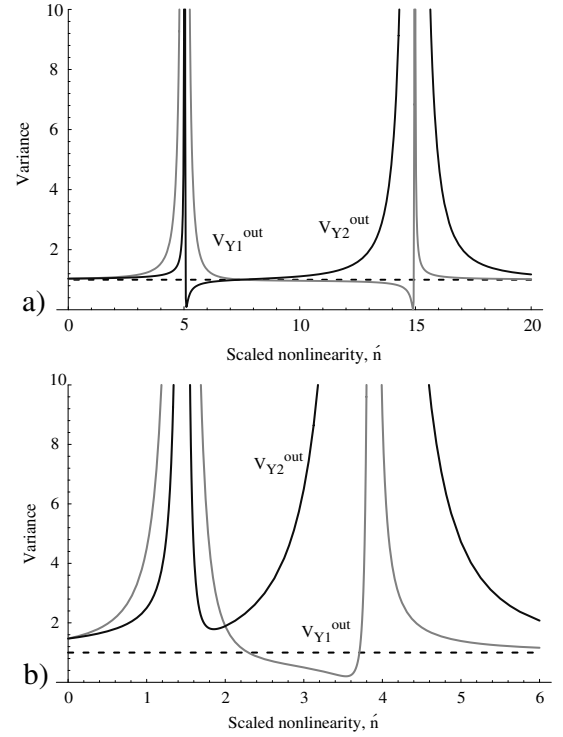

Figure 3. Y_1 and Y_2 quadratures versus scaled nonlinearity, $\acute{n} = \mu|\alpha_1|^2/\gamma_1$. The pump is quantum noise limited $V_{Y_1}^{\text{in1}}(\omega) = V_{Y_2}^{\text{in1}}(\omega) = 1$, the squeezing is observed at zero frequency, $\omega = 0$ for perfect outcoupling, $\acute{c} = \gamma_1^c/\gamma_1 = 1$ with: (a) scaled detuning $\acute{\Delta} = \Delta_1/\gamma_1 = 15$. Note that both quadratures are strongly squeezed, but at different values of the nonlinearity, (b) scaled detuning, $\acute{\Delta} = 5$, now only one quadrature is strongly squeezed.

$\omega = 0$, and, as always, optimum squeezing occurs when the intracavity squeezed field is output through only one port, i.e. $\gamma_1^c = \gamma_1$ and $\acute{c} = 1$, $\acute{\ell} = 0$. Under these conditions, the spectra become

$$V_{Y_{1,2}}^{2\psi}(0) = \Bigg([3 + (\acute{\Delta} - \acute{n})(\acute{\Delta} - 3\acute{n})]^2 V_{Y_{1,2}}^{\text{in1}}(0) + 4(\acute{\Delta} - \acute{n})^2$$

$$\times V_{Y_{2,1}}^{\text{in1}}(0)\Bigg) \Big/ \left\{[(\acute{\Delta} - \acute{n})(\acute{\Delta} - 3\acute{n}) + 1]^2\right\}. \qquad (12)$$

As figure 3(a) shows, in the limit where both the nonlinear and linear phase shifts are much greater than the cavity loss rate ($\mu|\alpha_1|^2$, $\Delta_1 \gg \gamma_1$), then both the Y_1 and Y_2 quadratures can be strongly squeezed (at different values of the nonlinearity naturally). However, as the phase shifts approach the value of the cavity loss ($\mu|\alpha_1|^2$, $\Delta_1 \sim \gamma_1$) the squeezing becomes less robust, and only the squeezing at the Y_2 quadrature survives, as shown in figure 3(b).

The frequency spectra of both quadratures for parameters where the Y_1 quadrature is near-perfectly squeezed are shown in figure 4(a). Even under these ideal conditions, the squeezing linewidth is relatively narrow (less than half the cavity linewidth), and there is considerable additional noise on the other quadrature. It is clear that even for ideal conditions, the Kerr squeezed states are not even close to being minimum uncertainty states.
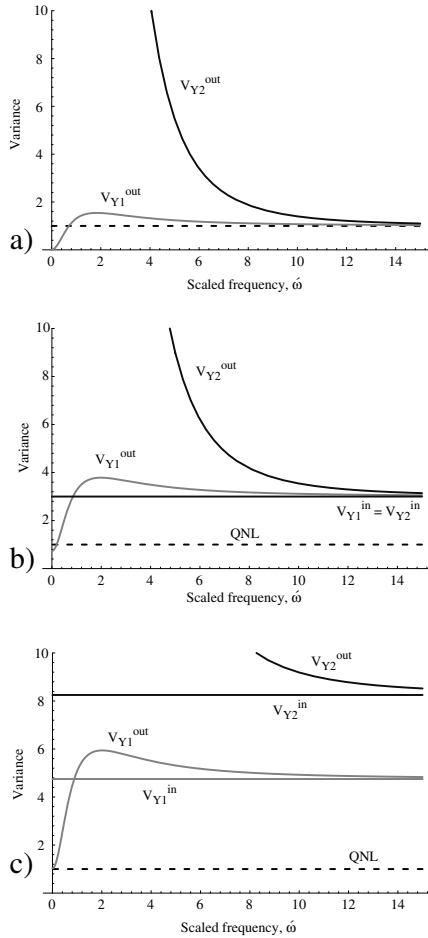
555

Figure 4. Theoretical Kerr squeezing spectra for Y_1, Y_2 quadratures. Scaled frequency, $\acute{\omega} = \omega/\gamma_1$; perfect outcoupling, $\acute{c} = 1$; scaled detuning $\acute{\Delta} = 15$; scaled nonlinearity such that $(\acute{\Delta} - \acute{n})(\acute{\Delta} - 3\acute{n}) = -3$; with: (*a*) quantum noise limited pump $V_{Y_1}^{\text{in1}}(\omega) = V_{Y_2}^{\text{in1}}(\omega) = 1$. Note the relatively narrow squeezing linewidth, (*b*) noisy pump $V_{Y_1}^{\text{in1}}(\omega) = V_{Y_2}^{\text{in1}}(\omega) = 3$. The squeezing is strongly degraded, but the output beam is still less noisy than the input beam on the Y_1 quadrature. This noise reduction is sometimes known as 'classical squeezing', (*c*) noisy pump $V_{X_1}^{\text{in1}}(\omega) = 3$, $V_{X_2}^{\text{in1}}(\omega) = 10$ observed at a quadrature angle $\theta = \pi/6$. The squeezing is destroyed, but the output beam is still less noisy than the input beam on the Y_1 quadrature.

2.2. The effects of driving noise

In the optimum case in SHG, the squeezing is influenced only by the amplitude quadrature of the driving field. As equations (12) makes clear, this is not the case for Kerr squeezing, where even in the optimum case both quadratures of the input field are coupled together and influence the output. In practical systems, the phase quadrature of laser light is typically noisier than the amplitude quadrature (at some frequencies many tens of dB more). In addition to noise from the same sources that contribute to the amplitude noise (relaxation oscillations, pump noise, spontaneous emission noise, etc) the phase quadrature suffers additional noise due to the intrinsic phase diffusion of the laser. Given its sensitivity to noise on both input quadratures, and that noise is ubiquitous in practical systems, it seems that the Kerr effect is inherently less advantageous than SHG as a robust source

of bright squeezed light. What exactly is the effect of extra phase quadrature noise on Kerr squeezing?

The noise spectra $V_{Y_1}^{\text{in1}}$ and $V_{Y_2}^{\text{in1}}$, are related to the amplitude and phase noise spectra, $V_{X_1}^{\text{in1}}$ and $V_{X_2}^{\text{in1}}$, by

$$
\begin{aligned}
V_{Y_1}^{\text{in1}} &= \cos^2(\theta) V_{X_1}^{\text{in1}} + \sin^2(\theta) V_{X_2}^{\text{in1}} \\
V_{Y_2}^{\text{in1}} &= \sin^2(\theta) V_{X_1}^{\text{in1}} + \cos^2(\theta) V_{X_2}^{\text{in1}}
\end{aligned}
\tag{13}
$$

where θ is the quadrature observation angle. Expressions for the amplitude quadrature noise for a four level laser, $V_{X_1}^{\text{in1}}(\omega)$, have been published and tested extensively against experiment [13, 26]. No equivalent expressions for the phase quadrature noise, $V_{X_2}^{\text{in1}}(\omega)$, currently exist, so we cannot yet produce detailed predictions to compare with experiment. Nevertheless, by assuming that the driving noise is white, we can tease out the chief effects of the noise fairly simply.

We consider the system of figure 4(*a*) except that now the output coupling is non-ideal, $\acute{c} = 0.6$ (similar to the experimental system considered later). If the system were driven with a quantum noise limited field then, solely due to the non-ideal coupling, we would expect perfect output squeezing to degrade from $V_{Y_1}^{\text{out1}}(\omega) = 0$ (100% squeezing) to $V_{Y_1}^{\text{out1}}(\omega) = 0.4$ (60% squeezing). Now consider driving the system with a uniformly noisy pump, $V_{X_1}^{\text{in1}}(\omega) = V_{X_2}^{\text{in1}}(\omega) = V_{Y_i}^{\text{in1}} = 3$ (i.e. 4.7 dB of white noise on all quadratures of the driving field). As shown in figure 4(*b*), the squeezing is further degraded, from $V_{Y_1}^{\text{out1}}(\omega) = 0.4$ (60% squeezing) to $V_{Y_1}^{\text{out1}}(\omega) = 0.8$ (20% squeezing): i.e. by a factor of 3 (4.7 dB). Note that although the reflected driving field is now only slightly squeezed, the Y_1 quadrature is considerably quieter than the that of the input field, over the approximately the same frequency range where it was squeezed when driven with a quantum noise limited field. This non-squeezed noise reduction of the driving field is sometimes known as 'classical squeezing' [23]. At high frequencies both quadratures asymptote to the input noise levels, since well away from the cavity resonance the cavity simply acts as a mirror.

So far, the behaviour of the Kerr system seems to parallel that of a similar SHG system, with the squeezing degradation straightforwardly linked to the amount of driving field noise. However, the behaviour is more complicated if the noise in the amplitude and phase quadratures of the driving field is unequal. Figure 4(*c*) considers (for the system of figure 4(*b*)), the case $V_{X_1}^{\text{in1}}(\omega) = 3$, $V_{X_2}^{\text{in1}}(\omega) = 10$ observed at the optimum angle, $\theta = \pi/6$: the squeezing is now totally destroyed. The classical noise reduction occurs over the same frequency range as previously, and in fact is is apparently stronger, as the input noise level has been raised. (However, in absolute terms the noise is reduced to approximately the same level as previously.) We conclude that, unlike SHG, in the Kerr effect large differences between the noise of the two quadratures quickly swamps the squeezing.

3. Experiment

As noted in the introduction, to date experimental exploration of these issues in the cw regime has been difficult, as the relatively weak $\chi^{(3)}$ nonlinearities of available optical

materials necessitated using atomic systems. However, in the past five years it was realized that cascading the much stronger $\chi^{(2)}$ nonlinearities of available optical materials can give a variety of effective third-order ($\chi^{(3)}$) effects [27, 28]. With the the experimental demonstration of a strong cascaded Kerr effect in a cw SHG system [22], a convenient experimental system exists for exploration of noise issues.

The cascaded Kerr effect may be understood as follows. Consider single-pass SHG in a lossless crystal of length L, driven by a fundamental beam of frequency ν. The light enters the crystal and begins to be strongly converted to the second harmonic at 2ν. However, the crystal is phase matched so that it has a coherence length of $L/2$, i.e. beyond this distance the second harmonic converts back to fundamental. The fundamental light exits the crystal with no change in power. However, as the light experiences a phase shift during both the SHG ($\nu \rightarrow 2\nu$) and OPO processes ($2\nu \rightarrow \nu$), and since the $\chi^{(2)}$ processes are nonlinear with intensity, so are the phase shifts: the total effect is an intensity dependent phase shift on the fundamental light, an effective Kerr effect.

3.1. Experimental system

In practice the effective Kerr effect is realized utilizing a cavity to build up the intensity of the fundamental field and thus increase the strength of the effect. Figure 5 shows the simplified experimental layout (the detailed experimental layout and techniques have been discussed elsewhere [13,25], and will not be given here). In brief, the system is driven by a diode pumped Nd:YAG ring laser (Lightwave 122) that produced a single mode at 1064 nm. A mode cleaning cavity acted as a low-pass filter to remove excess quadrature noise (both amplitude and phase) from the laser beam. The output of the mode-cleaner drove a monolithic cavity, which was a 12.5 mm long MgO:LiNbO$_3$ crystal with dielectric mirror coatings on the curved end faces ($R = 14.24$ mm). The monolith was singly resonant at the fundamental; the second harmonic executed a double-pass through the crystal, the second harmonic power could be varied by changing the phase matching of the crystal. Separate Pound–Drever locking schemes were used to lock the laser to the monolith, and the mode cleaner to the laser. The second harmonic was removed with a low-loss dichroic and sent to a balanced visible detector pair of quantum efficiency 90%; the reflected fundamental was accessed via the optical isolator and sent to a balanced infrared detector pair of quantum efficiency 80%. The propagation efficiency through the isolator and associated optics was approximately 63% so that the total quantum efficiency of the infrared detection setup was approximately 50%. The detuning was varied sinusoidally by modulating the locking point of the locking loop.

To investigate the phase matching of the monolith, the monolith was driven directly by the laser (the mode-cleaner was removed for simplicity), and the second harmonic power recorded. Figure 6 shows the phase-matching curve for a mode-matched input power of 33 mW. This curve is qualitative only: the temperature (measured via a thermocouple and thus given in volts) is not absolutely
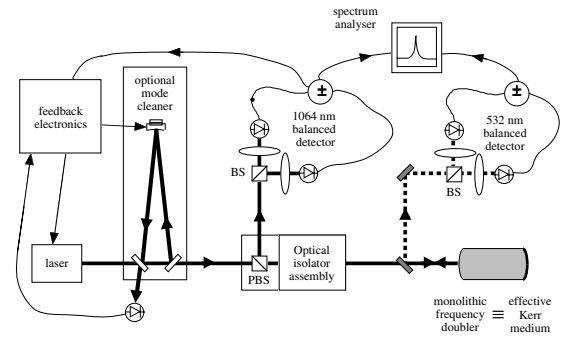

Figure 5. Simplified experimental layout. Details described in the text.
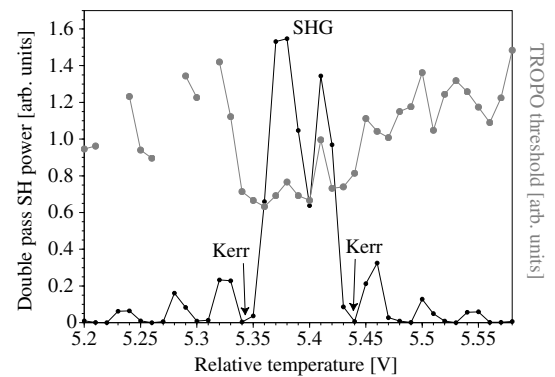

Figure 6. TROPO threshold and second harmonic power versus crystal realtive temperature. Lines are guides for the eye, but have been omitted when spanning temperatures where TROPO thresholds were not recorded. Note that the TROPO threshold varies little between the points of maximum (marked 'SHG') and minimum (marked 'Kerr') SHG.

calibrated, as it was used only to determine the relative phase-match settings where SHG and the Kerr effect occurred. Optimum second harmonic production occurred at thermocouple reading of 5.38 V, which corresponds to $\approx 110\,^{\circ}$C, where ± 0.05 V $\simeq \pm 0.5\,^{\circ}$C. The points of minimal second harmonic production immediately to the left (5.34 V) and right (5.44 V) of the maximum SHG are the Kerr points: it is at these points that strongly asymmetric cavity scans are observed when the system is pumped at high power. The monolith used in these experiments appears to suffer from less material inhomogeneities than that used in [22]: the phase-matching curve is symmetrical and less distorted; and the outcoupling ratio is some 10% higher (as inferred from the maximum SHG conversion efficiency of 60%). The linewidth of the cavity at room temperature is $\sim$10 MHz; at the Kerr points it is $\sim$10 MHz; and at the maximum SHG point it is broadened by the nonlinear loss $\sim$60 MHz (see [22, figure 5]).

Singly-resonant SHG systems are prone to a parasitic non-degenerate optical parametric oscillation pumped by the second harmonic, known as triply-resonant optical parametric oscillation, or TROPO. TROPO has been shown to add additional noise to the system, degrade squeezing, and clamp the second harmonic power [25], and is best avoided. Assuming that the parasitic signal and idler are simultaneously resonant with the fundamental, the minimum

power threshold power for TROPO is

$$P^{\min} = h(2\nu)\frac{\gamma_1^2}{\eta\mu}, \qquad (14)$$

which for our system was observed to be $P^{\min} \simeq 14$ mW at the phase-match point of maximum SHG production. This may seem irrelevant, as at the Kerr points minimal second harmonic is produced, (the nonlinearity is purely imaginary). However, considerable second harmonic was still produced within the cavity, and acted as a pump source: TROPO occurred at the Kerr points. The presence of TROPO (at powers above 20–30 mW) was detected via an infrared optical spectrum analyser. The TROPO threshold can be raised (and the TROPO suppressed for a given pump power) by temperature tuning the monolith: this affects the signal and idler so that they are not resonant with the fundamental, and decreases the nonlinearity. Unfortunately this only works to a limited extent in monolithic, type-I phase matched, systems (hemilithic and type-II systems are far more resistant to TROPO due to their intrinsically greater dispersion). Greatest suppression and highest threshold powers were achieved whilst scanning rapidly through resonance; shown in figure 6 are the measured thresholds whilst scanning. Note that the threshold is as low around the Kerr points as it is around the maximum SHG point. The TROPO thresholds dropped when the cavity was locked onto resonance, the signal and idler modes thermally 'pulled' themselves into resonance with the locked fundamental: when locked at the Kerr points, TROPO occurred for pump powers greater than 30 mW.

Power bistability occurs in Kerr systems when both the pump power and cavity detuning are greater than certain values. Due to their inherent instability, the regions near the bistability are obviously interesting points to investigate. In our system the degree of the Kerr effect is a function of the phase match, ΔkZ, thus the threshold power for bistability is given by [22]

$$P_1^{\text{bi thr}} = P_1^{\min} p(\Delta kZ), \qquad (15)$$

and the threshold detuning for bistability by

$$\Delta_1^{\text{bi thr}} = -\text{sign}(\text{Im } J)\frac{\sqrt{3}|\text{Im } J| + \text{Re } J}{|\text{Im } J| - \sqrt{3}\text{Re } J}\gamma_1, \qquad (16)$$

where $p(\Delta kZ)$ is the phase-match function

$$p(\Delta kZ) = \frac{2}{3\sqrt{3}}\frac{|J|^2}{(|\text{Im } J| - \sqrt{3}\text{Re } J)^3}, \qquad (17)$$

and J is

$$J = \frac{1}{2!} + \frac{\text{i}\Delta kZ}{3!} + \frac{(+\text{i}\Delta kZ)^2}{4!} + \cdots = \frac{\text{sinc}(\frac{\Delta kZ}{2})\text{e}^{-\text{i}\frac{\Delta kZ}{2}} - 1}{\text{i}\Delta kZ}. \qquad (18)$$

As shown previously, the SHG system acts as a pure Kerr cavity at the phase-match points $\Delta kZ = \pm n2\pi$, $n = 1, 2, \ldots$ [22]. We consider only the strongest effect, which occurs at the points $\Delta kZ = \pm 2\pi$: the power and detuning thresholds become $p(\Delta kZ) \simeq 2.4$ and $\Delta_1^{\text{bi thr}} = \sqrt{3}\gamma_1$. Regardless of the exact value of $p(\Delta kZ)$, equation (15) states

that the Kerr bistability threshold is always greater than the minimum TROPO threshold: to see bistability TROPO must be suppressed. Scanning through resonance at a rate of 12 MHz μs^{-1} suppressed TROPO, and bistable lineshapes were observed at high pump powers. However, as discussed above, when locked onto resonance the cavity could not be driven with more than 30 mW: above this TROPO occurred. Unfortunately this means that the cavity could not be driven into the bistable Kerr regime: TROPO is a major limitation of this particular system (monolithic, type-I phase matched).

3.2. Noise reduction

With the monolith phase matched for strong SHG production, and the mode-cleaner absent, moderate squeezing of the second harmonic was observed; with the introduction of the mode-cleaner, the second harmonic squeezing became much stronger [13]. (In neither case was significant squeezing expected or observed on the reflected fundamental.) Clearly the nonlinearity is strong enough for the production of squeezing. From [22] we expect the nonlinearity of the effective Kerr effect to be only a factor of π smaller than that of SHG: i.e. still large enough to cause noise reduction.

To investigate this, the monolith was set to the left Kerr point (5.34 V), and the mode-cleaner removed (for simplicity). When the laser was neither locked nor scanned, and detuned well away from the cavity resonance, the cavity acted as a simple reflector ($R > 99\%$). The spectrum of the reflected fundamental for this case is shown in figure 7 trace (a) (obtained from the sum port of the detector); figure 7 trace (b) is the quantum noise (obtained from the difference port of the detector). Clearly the laser beam is not quantum noise limited. The peak at 45 MHz is the residual amplitude noise from the phase modulation used in the Pound–Drever locking scheme. Considerable amplitude noise, due to the tail of the RRO of the laser [26], is evident at low-frequencies. Unless this low-frequency noise is removed (via the mode-cleaner) it will certainly mask any squeezing, as any squeezing produced will be at frequencies of the order of the cold cavity linewidth, i.e. ~ 10 MHz, and the pump noise extends beyond 20 MHz.

Next, the laser was brought onto resonance with the monolithic cavity, and locked. As the cavity was manually detuned the power of the reflected beam did not appreciably change (and the quantum noise trace was identical to trace (b)). However, the spectrum varied considerably: for most of the detuning range it was well above the original noise (as represented by trace (a)). However, for a narrow range of detunings the observed spectrum was quieter than the original light. Figure 7 trace (c) shows the spectrum for the optimum detuning. We stress that the reflected light is not squeezed (it is well above shot noise), but at low frequencies it is quieter than the original light by up to 1.5 dB. The extra structure around the locking peak highlights that we are no longer observing at the amplitude quadrature: due to the detuning we are somewhat rotated towards the phase quadrature, and are thus seeing more of the phase modulation. The noise reduction increased with increasing power. Unfortunately the power could not be increased past 30 mW as strong TROPO occurred.

Noise reduction and similar spectra were also observed for the right Kerr point (5.44 V), except that the optimum
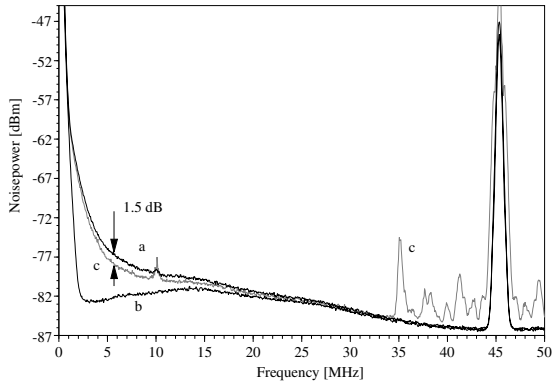
Figure 7. Reflected fundamental noise power versus frequency for Kerr cavity. (a) Noise from laser: measured on light reflected from cavity when laser is not locked, and detuned well away from resonance. The cavity thus acts as a simple mirror, $R > 99\%$. (b) Quantum noise for traces (a) and (c). (c) Noise on reflected beam at optimum detuning when crystal set to a Kerr point, i.e. phase-match conditions s.t. there is minimal second harmonic production, strongly asymmetric cavity scans, etc. For this plot, $T = 5.34$ V (cf $T = 5.38$ V, the point of optimum SHG squeezing).

noise reduction was then observed for a detuning of opposite sign to that of figure 7. This is a typical signature of a Kerr mechanism [22]. Noise reduction of the reflected fundamental only occurred in the vicinity of Kerr points. It was not observed when the crystal was set to the point of optimum SHG production ($\sim$60 MHz linewidth) nor at a temperature well away from SHG phase match, where no second harmonic was produced nor Kerr bistability observed ($\sim$10 MHz linewidth).

Ideally, the noise reduction versus quadrature of the reflected beam would be examined externally (with a homodyne detector, or cavity detector [10]), leaving the cavity properties fixed. Unfortunately neither option was available (due to limited power and components, respectively). So, to gain a feel for the detuning and quadrature dependence of the noise reduction at the Kerr points, the noise power was examined as the locked cavity was slowly detuned around resonance (the locking point was scanned at 298 mHz). The cavity could not be symmetrically detuned as the lineshape is bistable due to a thermal effect (which is quite independent of the unobtainable Kerr bistability, and occurs for all phase matches). On the stable side of the lineshape the cavity was detuned far enough that more than 90° of quadrature rotation was observed (the noise began to drop again). This suggests that the cavity was detuned on the order of 1 linewidth on that side of the lineshape. Figure 8 shows the noise power versus detuning at $f = 5.98$ MHz for the left Kerr point. Trace (a) is the simply reflected noise, as before; trace (b) is now the reflected noise as a function of detuning and trace (c) is the shot noise of the reflected light. The optimum noise reduction, 1.5 dB, occurs near, but not at, the peak of the lineshape (i.e. the minimum power of the reflected beam), which is itself shifted in detuning from the nominal zero detuning point of the cavity [22]. Beyond these observations, interpretation is necessarily proscribed as both the observed quadrature and degree of nonlinearity are affected by the detuning. However,
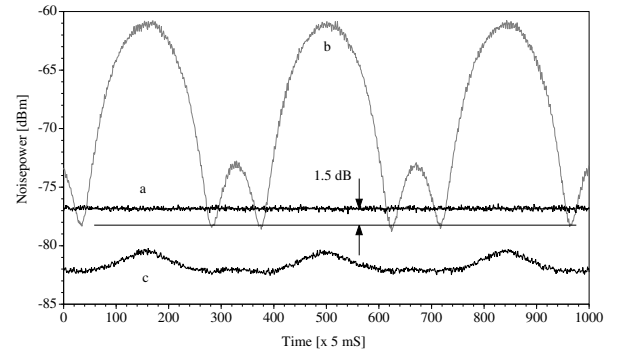

Figure 8. Reflected fundamental noise power versus frequency for Kerr cavity. (a) Noise from laser: measured on light reflected from cavity when laser is not locked, and detuned well away from resonance. The cavity thus acts as a simple mirror, $R > 99\%$. (b) Noise on reflected beam at 5.98 MHz as a function of detuning. $T = 5.34$ V, cf figure 7. (c) Quantum noise as a function of detuning, cf trace (b).
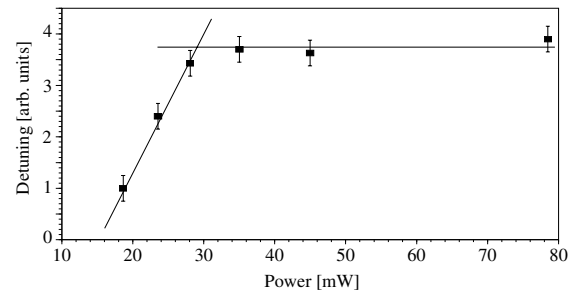

Figure 9. Optimum Kerr detuning (point of minimum noise) versus power, for $T = 5.34$ V. Above TROPO threshold the optimum detuning is clamped. Lines are guides for the eye only.

we can gain a relative feel for the quadrature rotation of the noise reduction by plotting detuning of the optimum noise reduction versus power, as shown in figure 9. The optimum detuning increases linearly with power, as expected, until $\sim$30 mW: above this, the optimum detuning is clamped, and does not vary greatly with power. This appears to be another signature of TROPO, as it coincided with the observed production of idler and signal modes, and is reminiscent of the second harmonic power clamping that occurs at the maximum SHG phase-match point [25].

In the SHG case, introduction of the mode cleaner non-trivially reduced the output noise: the classical noise was reduced, and the squeezing was increased. As figure 10 shows, in the Kerr case, introduction of the mode cleaner tivially reduced the output noise: classical noise was reduced, but no squeezing is observed. Why the difference?

Figure 10 is the quietest spectra, observed at the optimum detuning, which, as the raised noise between 28–42 MHz indicates, is near, but not at, the amplitude quadrature. The features at 45 and 27 MHz are the normal locking spikes from the monolith and mode-cleaner loops, respectively. The other features are beat signals and noise introduced by the dual locking loops, visible because we are not observing exactly at the amplitude quadrature. At these powers, the laser is quantum noise limited in the amplitude quadrature (as measured directly, and as inferred from the second harmonic amplitude squeezing), but the same is not true of the
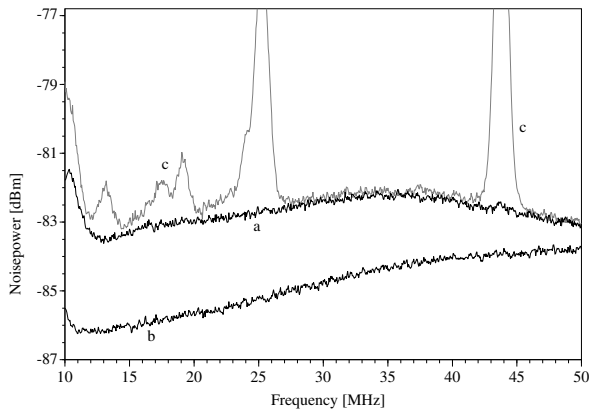
Figure 10. As for figure 7 but with mode-cleaner in place. No squeezing is seen, but there is considerable additional phase noise.

phase quadrature (there is additional phase noise even at low frequencies away from the induced technical noise). From our theoretical model, we saw that unbalanced amplitude and phase quadrature noises destroy squeezing (but still allow classical noise reduction). It is likely that, to some degree, this is happening here.

Note that there were technical problems specific to our experiment that further degraded performance. The TROPO intruded severely, limiting the maximum pump power and thus maximum noise reduction. The noise spikes below 20 MHz are signatures of a locking instability (caused by competition between the mode-cleaner and monolith locking loops) and this instability seeded the TROPO: with the mode-cleaner in place the monolith could not be driven above 20 mW without strong TROPO occurring. Finally, our total detector efficiency of 50% limited the maximum observable squeezing. These problems are specific to our particular experiment, not to effective Kerr systems in general. The TROPO problems could be straightforwardly overcome by using any high-dispersion doubler, such as the hemilithic frequency doubler commonly used as pump sources in OPO/A experiments [8, 9]. It appears that these hemilithic pump sources could be effective sources of squeezing in their own right.

4. Summary

In principle, when driven with quantum noise limited light, the Kerr medium has great value as a strong source of bright squeezed light. However, as the Kerr effect is intrinsically sensitive to fluctuations in both amplitude and phase, the Kerr effect is less robust than SHG if driven with noisy light. We developed a theory to quantify this sensitivity to driving noise, and found, in particular, that inequal values of amplitude and phase noise quickly destroys the squeezing. To test for this sensitivity, we used a nonlinear cavity that could be tuned between pure frequency doubler and pure Kerr behaviours. When set to be a frequency doubler, both classical noise reduction and squeezing were observed; when set to be a Kerr medium, classical noise reduction of 1.5 dB, but no squeezing, was observed on the reflected fundamental field. If using a Kerr medium for noise reduction, squeezing, or

quantum nondemolition, it is clear that care must be taken to ensure that the pump beam is as close to shot noise limited as achievable, or failing that, at least equally noisy in both quadratures. A strong Kerr effect can be realized by cascading $\chi^{(2)}$ nonlinearities, however, to fulfil their noise reduction potential such systems should be made highly dispersive, to suppress unwanted parametric oscillation.

References

[1] Slusher R E, Hollberg L W, Yurke B, Mertz J C and Valley J F 1985 *Phys. Rev. Lett.* **55** 2409
[2] Xiao M, Wu L A and Kimble H J 1988 *Opt. Lett.* **13** 476
Marin F, Bramati A, Jost V and Giacobino E 1997 *Opt. Commun.* **140** 146
Kasapi S, Lathi S and Yamamoto Y 1997 *Opt. Lett.* **22** 478
Furusawa A, Sorensen J L, Braunstein S L, Fuchs C A, Kimble H J and Polzik E S 1998 *Science* **282** 706
Ralph T C and Lam P K 1998 *Phys. Rev. Lett.* **81** 5668
[3] Bergman K and Haus H A 1991 *Opt. Lett.* **16** 663
Bergman K, Haus H A, Ippen E P and Shirasaki M 1994 *Opt. Lett.* **19** 290
[4] Friberg S R, Machida S, Werner M J, Levanon A and Mukai T 1996 *Phys. Rev. Lett.* **77** 3775
[5] Schmitt S, Ficker J, Wolff M, Knig F, Sizmann A and Leuchs G 1998 *Phys. Rev. Lett.* **81** 2446
[6] Marin F, Bramati A, Giacobino E, Zhang T C, Poizat J-Ph, Roch J F and Grangier P 1995 *Phys. Rev. Lett.* **75** 4606
[7] Inoue S, Lathi S and Yamamoto Y 1997 *J. Opt. Soc. Am.* B **14** 2761
Zhang T C, Poizat J-Ph, Grelu P, Roch J F, Grangier P, Marin F, Bramati A, Jost V, Levenson M D and Giacobino E 1995 *Quantum Semiclass. Opt.* **7** 601
[8] Lam P K, Ralph T C, Buchler B C, McClelland D E, Bachor H-A and Gao J 1999 *J. Opt. B: Quantum Semiclass. Opt.* at press
[9] Schneider K, Bruckmeier R, Schiller S and Mlynek J 1996 *Opt. Lett.* **21** 1396
[10] Galatola P, Lugiato L A, Porreca M G, Tombesi P and Leuchs G 1991 *Opt. Commun.* **85** 95
[11] Pereira S F, Ou Z Y and Kimble H J 1994 *Phys. Rev. Lett.* **72** 214
[12] Ralph T C, Taubman M S, White A G, McClelland D E and Bachor H-A 1995 *Opt. Lett.* **20** 1316
[13] White A G, Taubman M S, Ralph T C, Lam P K, McClelland D E and Bachor H-A 1996 *Phys. Rev.* A **54** 3400
[14] Tsuchida H 1995 *Opt. Lett.* **20** 2240
[15] Ralph T C and White A G 1995 *J. Opt. Soc. Am.* B **12** 833
[16] Lambrecht A, Courty J M, Reynaud S and Giacobino E 1995 *Appl. Phys.* B **60** 129
Lambrecht A, Coudreau T, Steinberg A M and Giacobino E 1996 *Europhys. Lett.* **36** 93
[17] Hope D M, Bachor H-A, Manson P J, McClelland D E and Fisk P T H 1992 *Phys. Rev.* A **46** R1181
Hope D M, McClelland D E, Bachor H-A and Stevenson A J 1992 *Appl. Phys.* B **55** 210
[18] Raizen M G, Oroczo L A, Xiao M, Boyd T L and Kimble H J 1987 *Phys. Rev. Lett.* **59** 198
Orozco L A, Raizen M G, Xiao M, Brecha R J and Kimble H J 1987 *J. Opt. Soc. Am.* B **4** 1490

[19] Drummond P D and Walls D F 1980 *J. Phys. A: Math. Gen.* **13** 725

[20] Collett M J and Walls D F 1985 *Phys. Rev.* A **32** 2887

[21] Reynaud S, Fabre C, Giacobino E and Heidmann A 1989 *Phys. Rev.* A **40** 1440

[22] White A G, Schiller S and Mlynek J 1996 *Europhys. Lett.* **35** 425

[23] Bachor H-A 1998 *A Guide to Experiments in Quantum Optics* 1st edn (Weinheim: Wiley)

[24] Walls D F and Milburn G J 1994 *Quantum Optics* 1st edn (Berlin: Springer)

[25] White A G, Lam P K, Taubman M S, Marte M A M, Schiller S, McClelland D E and Bachor H-A 1997 *Phys. Rev.* A **55** 4511–5

[26] Ralph T C, Harb C C and Bachor H-A 1996 *Phys. Rev.* A **54** Harb C C, Ralph T C, Huntington E H, Freitag I, McClelland D E and Bachor H-A 1996 *Phys. Rev.* A **54** 4370

[27] For example, see references in Assanto G, Stegeman G I, Sheik-Bahae M and VanStryland E 1995 *J. Quantum Electron.* **31** 673

[28] Stegeman G, Shei-Bahae M, Van Stryland E W and Assanto G 1993 *Opt. Lett.* **18** 13